arXiv:1402.1264v1 [physics.atom-ph] 6 Feb 2014

Relativistic coupled cluster calculations on hyperfine structures and electromagnetic transition amplitudes of In III

Sourav Roy, Narendra Nath Dutta and Sonjoy Majumder
Department of Physics, Indian Institute of Technology-Kharagpur, Kharagpur-721302, India

(Dated: February 7, 2014)

Hyperfine constants and anomalies of ground as well as few low lying excited states of ^{113,115,117}In III are studied with highly correlated relativistic coupled-cluster theory. The ground state hyperfine splitting of ^{115}In III is estimated to be 106.8 GHz. A shift of almost 1.9 GHz of the above frequency has been calculated due to modified nuclear dipole moment. This splitting result shows its applicability as communication band and frequency standards at 10^{-11} sec. Correlations study of hyperfine constants indicates a few distinct features of many-body effects in the wave-functions in and near the nuclear region of this ion. Astrophysically important forbidden transition amplitudes are estimated for the first time in the literature to our knowledge. The calculated oscillator strengths of few allowed transitions are compared with recent experimental and theoretical results wherever available.

I. INTRODUCTION

Recent trapping of doubly ionized Yb [1] can enhance the possibility of the trapping of doubly ionized In using the same experimental mechanism. Trapped ^{113}Cd II is known as an ideal candidate for the frequency standard and quantum computing [2, 3]. Being in the same Ag-isoelectronic sequence, ^{113,115,117}In III is further interesting from the point of view due to its expected large hyperfine splitting like ^{113}Cd$^+$ as it is next to the latter ion in this sequence, has nuclear g-factor close to that of ^{113}Cd and has large nuclear spin (I=4.5 for all these In isotopes, but I=1.5 for ^{113}Cd). The discrepancies between experimental [4–6] and theoretical [7, 8] estimations of magnetic dipole hyperfine constants of ^{115}In I indicate the possibility of small variation of nuclear moment obtained from Raghavan et al.[9]. This is, however, very important for the nuclear theory and physics where precise nuclear parameters are important, like PNC estimations [10–12]. The study of nuclear magnetization distribution on the indium isotopes has been an interesting topic from the point of its "puzzling giant hyperfine anomaly"[13–15]. The magnetic property can be estimated from their hyperfine anomalies (Bohr-Weisskopf effect only[16, 17]). These are calculated using accurate estimations of the hyperfine splitting of states. Study of this anomaly over different level of atomic ionizations provides the ionization effect on the nucleus. The results obtained should provide a useful calibration for nuclear theory as well as they reduce limitations of precise measurement of fundamental constants, like parity and/or time violation constants, due to the uncertainty of neutron distribution [12, 18].

Strong resonance lines from In III are required in order to provide the most important data for abundance analysis in various astronomical systems as well as laboratory plasmas [19–22]. Explanation of the observed large discrepancies between experimental[23, 24] and theoretical[25] line broadening results in the optical spectrum [23] of In III requires precise estimations of allowed transitions. Also, the forbidden transitions are the effective decay mechanism in low density hot plasmas where the possibility of collisional de-excitation is low [26]. There have been many experimental and theoretical endeavor of estimating the strengths of some ultraviolet or visible lines of this ion over the years [27–34]. However, due to the large discrepancies among the results, it is required to have correlation exhaustive relativistic ab initio calculations. Also, we augment the database with lifetime of few other low lying states. Some of these are estimated for the first time in the literature to our knowledge.

Here, we have employed highly correlated relativistic coupled-cluster (RCC) method based on the Dirac-Coulomb-Gaunt Hamiltonian to generate the ground and different excited states [35] of In III. With respect to the other well known theories, the coupled cluster theory has the potential of taking electron correlation in an exhaustive way [3, 36]. The various kind of many body effects like core correlation, core polarization and pair correlation are also studied in the framework of the present RCC theory in the calculations of the hyperfine constants.

II. THEORY

In order to obtain a correlated wave-function $|\Psi_v\rangle$ corresponding to a single valence atomic state having valence electron in 'v'th orbital, one need to solve the corresponding energy eigen-value equation where Dirac-Coulomb-Gaunt Hamiltonian is considered[35]. In the coupled-cluster theory, one can write this correlated wave-function as [3, 36–39],

$$|\Psi_v\rangle = e^T\{1 + S_v\}|\Phi_v\rangle \qquad (2.1)$$

Here, $|\Phi_v\rangle$ is the Dirac-Fock reference state wave-function which is generated in the V^{N-1} potential following Koopman's theorem [40]. T is the closed-shell cluster operator which takes all the single,

double, and so on excitations from the core orbitals [36]. S_v is the open-shell cluster operator which behaves as T but excites atleast one electron from the valence 'v'[36].

The general matrix element of an operator $\hat{O}$ can be conveniently expressed with normalization as,

$$O_{fi} = \frac{\langle \Psi_f | \widehat{O} | \Psi_i \rangle}{\sqrt{\langle \Psi_f | \Psi_f \rangle \langle \Psi_i | \Psi_i \rangle}} \tag{2.2}$$

The single particle reduced matrix elements of the electric dipole ($E1$), electric quadrupole ($E2$), magnetic dipole ($M1$) transition operators and the operators associated with the magnetic dipole (A) and electric quadrupole hyperfine (B) constants are given in Ref. [41].

The hyperfine anomaly due to BohrWeisskopf effect for any particular state is defined by the following expression [14, 42]

$$\Delta\% = \frac{A_1 g_2 - A_2 g_1}{A_2 g_1} \times 100 \tag{2.3}$$

where, A_1, A_2 are the hyperfine constants and g_1, g_2 are the corresponding g-factors of the nuclei, of the isotopes of concern.

III. RESULTS AND DISCUSSIONS

The procedure of generating the DF orbital bases for the correlated RCC wavefunctions used in the present calculations has been discussed earlier [41, 43]. In the present work, the percentage value in the correlation contribution (RCC result − DF result) is defined with respect to the DF result. In Table I, we represent ionisation potentials (IPs) of the ground state and few low lying excited states in cm^{-1}. Our RCC results are compared with the experimental values obtained from the National Institute of Standards and Technology (NIST) [44]. The maximum difference among these values occurs in the case of $4f\ ^2F_{5/2}$ state, which is about 0.44 %.

In Table II, we present the $E1$ transition amplitudes in the length gauge form at the DF and the RCC levels. The correlation contributions (Corr) are presented in the same table. The wavelengths of these transitions which are calculated from the IPs of NIST are quoted at the second column of this table. The correlation effect decreases the transition amplitudes in all the cases except the transition $5s\ ^2S_{1/2} \rightarrow 6p\ ^2P_{1/2}$. We get correlation contribution is much larger than DF values for $5s\ ^2S_{1/2} \rightarrow 6p\ ^2P_{1/2,3/2}$ transitions unlike to the other cases[33]. These have been also observed in velocity gauge calculations. The two resonance transitions $5s\ ^2S_{1/2} \rightarrow 5p\ ^2P_{1/2,3/2}$ are about -17.2 % to -17.5 % correlated and it has been estimated that most of their correlations come from the core polarization effect. The core polarization is also found to be the dominating mechanism in the transitions $5p\ ^2P_{3/2} \rightarrow 5d\ ^2D_{3/2,5/2}$ and $5p\ ^2P_{1/2} \rightarrow 5d\ ^2D_{3/2}$ where total correlation contributions are about -11.8 % to -12.2 %. The oscillator strengths of $E1$ transitions calculated from the corresponding transition amplitudes and quoted wavelengths are also presented in Table II. These transitions are astrophysically important [20] and fall in the visible and ultraviolet regions of electromagnetic spectrum.

Table II also shows the discrepancies among various theoretical and experimental results. Our highly correlated *ab initio* calculations show excellent agreement with the model potential [45] and RMBPT calculations [30]. Here, the experimental results are evaluated from the corresponding lifetime measurements [29, 46] and NIST wavelengths [44]. Considerable differences are noted from the experimentally measured values with all the theoretical results for the $5p\ ^2P_{1/2} \rightarrow 5d\ ^2D_{3/2}$ and $5p\ ^2P_{3/2} \rightarrow 6s\ ^2S_{1/2}$ transitions. Therefore, more precise experiments are desirable for these cases. Also recent experiment [23] claims accurate estimations of absorption coefficients of 298.28, 300.808 and 524.877 nm transition lines where our calculated amplitudes can be used.

Though electromagnetically forbidden transitions do not contribute significantly to the lifetimes of the excited states here, they are important in different areas of physics [41]. There has been calculation of magnetic dipole ($M1$) transition rate between the fine-structure states of $4f\ ^2F$ using multi-configuration Dirac-Fock (MCDF) method [34]. Our calculated fine-structure splitting (-23 cm^{-1}) of this term is much closure to the central experimental value (8 cm^{-1})[44] compare to the MCDF calculation (-71 cm^{-1}). The latter calculation estimated comparatively large correlation contribution as the DF value is -24 cm^{-1}. There is a discrepancy between the MCDF and our calculations of transition amplitude between these fine structure states. where former is evaluated from their calculated transition probability and wavelength. Most probably, the discrepancy can be avoided with proper choice of initial and final states and use of NIST wavelength[44].

The $E2$ and $M1$ transition amplitudes along with their corresponding NIST wavelengths (λ-values) are presented in the Table III. The correlation contributions (corr) to all the $E2$ transitions reduce the corresponding DF-values and vary from -4.9 % to -9.3 %. The $5s\ ^2S_{1/2} \rightarrow 5d\ ^2D_{3/2,5/2}$ transitions are maximally correlated by -9.2 % to -9.3 % with respect to all others E2 transitions presented here. It has been observed (see Fig. 1)that M1 transition probabilities are stronger than E2 probabilities for transition among fine structure states.

In Table IV, we compare our calculated life times for some low lying states with the other theoretically calculated and experimentally measured values. Lifetimes of few states are presented in this table for the first time in the literature to our

knowledge. The experimental wavelengths from the NIST are used in our calculations. The beam foil experiment of Andersen et al.[29] and the relativistic Hartree Fock (RHF) calculation [32] of Cheng et at. underestimate the lifetime of the $5p\ ^2P_{1/2}$ state. Our estimated life times are in good agreement with the measured values of Ansbacher et al. [46] and calculated results as obtained using the RMBPT method [30], except in the case of $5d\ ^2D_{3/2}$ state. The lifetime of the $5d\ ^2D_{3/2}$ state measured by the beam foil experiment [46] and calculated by the RMBPT method are 0.75 ± 0.06 and 0.67 nanosecond, respectively. These lifetimes are based only on the transition $5d\ ^2D_{3/2} \rightarrow 5p\ ^2P_{1/2}$. Whereas, considering both the channels of emissions $5d\ ^2D_{3/2} \rightarrow 5p\ ^2P_{1/2}$ and $5d\ ^2D_{3/2} \rightarrow 5p\ ^2P_{3/2}$, our RCC calculations yields this lifetime 0.53×10^{-9} sec. Similar arguments also hold in the comparison of the lifetimes of the $4f\ ^2F_{5/2}$ state, where our calculations considered all the channels of emissions compare to the other results which account emission through only the dominating channel. However, for $5d\ ^2D_{5/2}$ state there is only one dominating channel $5d\ ^2D_{5/2} \rightarrow 5p\ ^2P_{3/2}$ and we, therefore, find good agreement with experiment[46]. Anderson et al. also overestimates the lifetime of this state. The corrections due to the $E2$ and/or $M1$ transitions in the calculations of all the lifetime values come at or beyond the four decimal place in the unit of nanosecond. This may be important for ultra-fast spectroscopy[48].

The accurate estimation of the large hyperfine splitting of the ground state of ^{115}In III is one of the most important objectives of this work. The magnetic dipole and the electric quadrupole moments of the stable ^{115}In isotope are considered 5.5408(2) nuclear magnetons and +0.810 barns, respectively from Ref. [9] with nuclear spin-parity $9/2^+$. In Table V, the hyperfine A-constants of the ground and few excited states are presented at the DF and RCC levels along with the contributions of different correlation terms. In this table, $\overline{d} = e^{T^\dagger} d e^T$ represents the sum of DF (d) and core correlation contribution. According to the RCC theory, the lowest order pair correlation and core polarization effects arise from the terms $\overline{d}S_1$+c (indicated by $\overline{d}S_1$ in the table) and $\overline{d}S_2$+c (indicated by $\overline{d}S_2$ in the table), respectively, where c stands for the conjugate term [35]. These effects are presented in Table V along with some significantly contributing terms like $S_1^\dagger \overline{d} S_1$, $S_1^\dagger \overline{d} S_2$+c (indicated by $S_1^\dagger \overline{d} S_2$ in the table) and $S_2^\dagger \overline{d} S_2$. Here, 'Norm' represents the normalization correction[47]. The largest correlation contributions come from the pair correlation terms for the $5s\ ^2S_{1/2}$, $5p\ ^2P_{1/2,3/2}$ and $6p\ ^2P_{1/2}$ states. Whereas, the core polarization contributes the most to the $6s\ ^2S_{1/2}$, $7s\ ^2S_{1/2}$, $5d\ ^2D_{3/2,5/2}$, $6p\ ^2P_{3/2}$ and $4f\ ^2F_{5/2,7/2}$ states. These are graphically presented in Fig. 2. It is also clear from the Fig. 2 that the pair correlation contributions are decreasing to the outer orbitals along the same relativistic symmetry, which is expected[50]. The percentage of pair correlation contributes almost identically for the fine-structure states of any term has also been observed. $4f\ ^2F_{5/2}$ and $4f\ ^2F_{7/2}$ states show large percentage of negative core polarization contributions. These large negative contributions dominantly arise from the exchange part of these correlation terms. The A-constants of the low-lying bound $ns\ ^2S_{1/2}$ states fall in the GHz range and their high values are expected due to the large overlap of their wave functions in the nuclear vicinity. The total correlation contribution to the A-constant of the ground state is around 20.9 %. The estimated hyperfine A constants of all these states are presented within an approximate theoretical uncertainty of ± 2 %.

Our calculated hyperfine B-constants for the low lying states are presented in Table VI along with the different correlation contributing many body terms. In this table, the labelling of the different terms are done identically as those are done in Table V. The percentage values of the total correlation contributions to these A and B constants are plotted in Fig. 3 to get an idea about their relative responses. The correlation to the $4f\ ^2F$-states shows an opposite trends between these two constants. This may be a consequence of difference of the behaviour of the wavefunctions in two different radial regions of nuclear proximity. Here, one can see that the core polarization contributes strongly to all the cases with respect to the other correlation terms. This is clear from Table VI and Fig. 4. Even, the RCC values of the $5d\ ^2D_{3/2,5/2}$ states become more than twice of their corresponding DF values due to large core polarization effects. The correlation contributions to the hyperfine B constants of the $4f\ ^2F_{5/2,7/2}$ and $5g\ ^2G_{7/2,9/2}$ states change abnormally from the DF to the RCC levels. These abnormal changes are also guided by the core polarization effects. One can also find from Fig. 4 that the percentage contribution of the core polarization is almost same to the fine-structure states of a term.

The hyperfine splitting of the ground as well as few low lying excited states are presented in Table VII. The percentage contributions from the B-constants to the splitting values are presented at the last column of this table. The comparison of theoretically estimated [7] and experimentally measured [4] hyperfine constants of different states shows nuclear magnetic moment may be 5.4422 μ_B for ^{115}In I. This value varies from the standard value as obtained from Raghavan et al. by 5.5408 μ_B [9]. This changes the ground state splitting by 0.0634 cm^{-1}, which is substantial in terms of accuracy we are looking for.

Study of Nuclear magnetization distribution (NMD) of any atomic system provides informations about nuclear wave functions, which is very

TABLE I. IPs of ground and low-lying excited states in cm^{-1}

State	RCC	NIST
$5s\ ^2S_{\frac{1}{2}}$	226445.34	226191.3
$5p\ ^2P_{\frac{1}{2}}$	168645.05	169010.2
$5p\ ^2P_{\frac{3}{2}}$	164208.93	164668.1
$6s\ ^2S_{\frac{1}{2}}$	99353.88	99317.1
$5d\ ^2D_{\frac{3}{2}}$	97713.82	97738.5
$5d\ ^2D_{\frac{5}{2}}$	97288.94	97448.8
$6p\ ^2P_{\frac{1}{2}}$	81409.35	81607.7
$6p\ ^2P_{\frac{3}{2}}$	80011.96	80268.7
$4f\ ^2F_{\frac{5}{2}}$	63937.80	64222.5
$4f\ ^2F_{\frac{7}{2}}$	63960.98	64214.5
$7s\ ^2S_{\frac{1}{2}}$	56699.72	56761.5
$5g\ ^2G_{\frac{7}{2}}$	39497.11	39669.3
$5g\ ^2G_{\frac{9}{2}}$	39497.11	39669.3

important for the PNC calculations[18]. It is difficult to measure the nuclear magnetization distribution (NMD) experimentally[18, 49], rather it can be estimated from accurate value of hyperfine splitting using Bohr-Weisskoff formalism [14]. Though mean contribution of this effect appears only for $S_{1/2}$ and $P_{1/2}$ states, but other states, like $P_{3/2}$, are effected due to $e^- - e^-$ interaction. Using Eq(2.3), we have calculated hyperfine anomaly of In III isotopes between 113 and 115 ($^{113}\Delta^{115}(\%)$) and 115 and 117 ($^{115}\Delta^{117}(\%)$). We present these results in Table VIII. Like neutral Indium, we observe considerable effect of finite nucleus in these parameters for In III[42]. However, we do not see significant changes in the parameter between $P_{1/2}$ and $P_{3/2}$-states as was observed in neutral system[14, 42].

A. Conclusion

The electro-magnetic transition amplitudes, lifetimes and hyperfine constants are calculated using a highly correlated theoretical approach with a proper account of relativity. Our calculated transition line parameters can be applied for abundance estimations in different astronomical systems and laboratory plasmas. The ground state hyperfine splitting of this ion predicts its use as microwave frequency standard at 10^{-11} sec. The detail analysis of the different correlation contributing terms associated with the coupled-cluster theory show their impacts in the calculations of the hyperfine constants. The hyperfine B constants of the fine structures of $4f\ ^2F$ and $5g\ ^2G$ terms are found to be abnormally correlated due to the very strong influence of the core polarization. The calculated hyperfine splitting can be used for accurate line-profile analysis of astrophysically important transition lines. We have also observed distinct feature in the hyperfine anomaly parameters compare to neutral Indiun.

ACKNOWLEDGMENTS

We are thankful to Prof. B. P. Das and Dr. R. K. Choudhuri, IIA, Bangalore, India and Dr. B. K. Sahoo, PRL, Ahmedabad, India for providing the COUPLED-CLUSTER code to us. We also want to acknowledge Board of Research in Nuclear Sciences (BRNS), India; for funding.

TABLE II. Calculated E1 transition amplitudes (in a.u.) and oscillator strengths. The corresponding wavelengths (λ) are presented in Å. The oscillator strengths calculated by other theory and experimental measurements (Expt) are also reported for comparison with our relativistic coupled-cluster (RCC) results.

		Transition amplitudes			Oscillator Strengths		
Transitions	λ	DF	Corr	RCC	RCC	Other theory	Expt
$5s\ ^2S_{1/2} \rightarrow 5p\ ^2P_{1/2}$	1748.83	2.0868	-0.3656	1.7212	0.2600	0.2519[a],0.260[b]	0.27[c],0.2796[d]
						0.260[e],0.1963[f]	
						0.2486[g]	
$\rightarrow 5p\ ^2P_{3/2}$	1625.40	2.9512	-0.5070	2.4442	0.5647	0.5478[a], 0.567[b]	0.60[c],0.5279[d]
						0.278[e],0.4248[f]	
						0.5400[g]	
$\rightarrow 6p\ ^2P_{1/2}$	691.64	0.0324	0.1130	0.1454	0.0047	0.0003[f]	
$\rightarrow 6p\ ^2P_{3/2}$	685.30	0.0403	-0.1653	-0.1250	0.0035	0.0007[f]	
$5p\ ^2P_{1/2} \rightarrow 6s\ ^2S_{1/2}$	1434.86	1.2795	-0.0473	1.2322	0.1598	0.161[b]	
$\rightarrow 5d\ ^2D_{3/2}$	1403.08	3.3519	-0.4100	2.9419	0.9323	0.9113[a],0.900[b]	0.7870[d]
$\rightarrow 7s\ ^2S_{1/2}$	890.88	0.3917	-0.0031	0.3886	0.0257		
$5p\ ^2P_{3/2} \rightarrow 6s\ ^2S_{1/2}$	1530.20	1.9776	-0.0774	1.9002	0.1778	0.179 [b]	0.2506[d]
$\rightarrow 5d\ ^2D_{3/2}$	1494.11	1.5574	-0.1837	1.3737	0.0954	0.0932[a],0.092[b]	
$\rightarrow 5d\ ^2D_{5/2}$	1487.67	4.6559	-0.5481	4.1078	0.8575	0.8387[a],0.831[b]	0.8585[d]
$\rightarrow 7s\ ^2S_{1/2}$	926.73	0.5786	-0.0095	0.5691	0.0265		
$6s\ ^2S_{1/2} \rightarrow 6p\ ^2P_{1/2}$	5646.72	4.3068	-0.2107	4.0961	0.4573	0.3708[f]	
$\rightarrow 6p\ ^2P_{3/2}$	5249.79	6.0411	-0.2907	5.7504	0.9714	0.7884[f]	
$5d\ ^2D_{3/2} \rightarrow 6p\ ^2P_{1/2}$	6199.32	4.1135	-0.1120	4.0015	0.1983		
$\rightarrow 6p\ ^2P_{3/2}$	5724.16	1.7862	-0.0453	1.7409	0.0407		
$\rightarrow 4f\ ^2F_{5/2}$	2983.65	7.0372	-0.4556	6.5816	1.1110	1.0915[a]	1.1771[d]
$5d\ ^2D_{5/2} \rightarrow 6p\ ^2P_{3/2}$	5820.69	5.4252	-0.1366	5.2885	0.2446		
$\rightarrow 4f\ ^2F_{5/2}$	3009.66	1.8915	-0.1213	1.7702	0.0529	0.0520[a]	
$\rightarrow 4f\ ^2F_{7/2}$	3008.94	8.4595	-0.5422	7.9173	1.0711	1.0394[a]	1.0522[d]
$6p\ ^2P_{1/2} \rightarrow 7s\ ^2S_{1/2}$	4024.76	2.7944	-0.0806	2.7138	0.2764		
$6p\ ^2P_{3/2} \rightarrow 7s\ ^2S_{1/2}$	4254.02	4.2633	-0.1228	4.1405	0.3035		

$a, g \rightarrow$ Third-order Relativistic Many-Body Perturbation Theory (RMBPT): [30, 51];
$b \rightarrow$ Core Polarized augmented Dirac-Fock method (DF+CP): [45];
$c \rightarrow$ Beam Foil technique : [29];
$d \rightarrow$ Beam Foil technique: [46];
$e \rightarrow$ Configuration Interaction calculation(CI): [31];
$f \rightarrow$ Relativistic Quantum Defect Orbital method(RQDO): [33];

TABLE III. Calculated $E2$ and $M1$ transition amplitudes in a.u.. The corresponding wavelengths (λ) are presented in Å

		$E2$			$M1$		
Transitions	λ	DF	Corr	RCC	DF	Corr	RCC
$5s\ ^2S_{1/2} \rightarrow 5d\ ^2D_{3/2}$	778.50	6.8096	-0.6241	6.1855			
$\rightarrow 5d\ ^2D_{5/2}$	776.74	8.3060	-0.7744	7.5316			
$5p\ ^2P_{1/2} \rightarrow 5p\ ^2P_{3/2}$	23030.33	8.7362	-0.7523	7.9839	1.1532	0.0001	1.1533
$\rightarrow 6p\ ^2P_{3/2}$	1126.87	5.1577	-0.4127	4.7450	0.0317	0.0011	0.0328
$\rightarrow 4f\ ^2F_{5/2}$	954.31	11.5617	-1.0246	10.5371			
$5p\ ^2P_{3/2} \rightarrow 6p\ ^2P_{1/2}$	1203.94	6.1114	-0.4543	5.6571	0.0336	0.0008	0.0344
$\rightarrow 6p\ ^2P_{3/2}$	1184.84	5.7550	-0.4327	5.3223	0.0003	0.0006	0.0009
$\rightarrow 4f\ ^2F_{5/2}$	995.56	6.5714	-0.5601	6.0113			
$\rightarrow 4f\ ^2F_{7/2}$	995.48	16.1049	-1.3733	14.7316			
$6s\ ^2S_{1/2} \rightarrow 5d\ ^2D_{3/2}$	63347.27	20.8068	-1.1669	19.6399			
$\rightarrow 5d\ ^2D_{5/2}$	53524.59	25.7109	-1.4279	24.2830			
$5d\ ^2D_{3/2} \rightarrow 5d\ ^2D_{5/2}$	345184.67	12.5903	-0.8226	11.7677	1.5491	0.0001	1.5492
$\rightarrow 7s\ ^2S_{1/2}$	2440.39	6.9372	-0.3581	6.5791			
$5d\ ^2D_{5/2} \rightarrow 7s\ ^2S_{1/2}$	2457.77	8.7467	-0.4355	8.3112			
$6p\ ^2P_{1/2} \rightarrow 6p\ ^2P_{3/2}$	74682.60	37.2585	-2.0824	35.1762	1.1531	0.0000	1.1531
$\rightarrow 4f\ ^2F_{5/2}$	5752.02	40.9209	-2.2989	38.6220			
$6p\ ^2P_{3/2} \rightarrow 4f\ ^2F_{5/2}$	6232.01	22.1480	-1.2351	20.9129			
$\rightarrow 4f\ ^2F_{7/2}$	6228.90	54.1958	-3.0186	51.1772			
$4f\ ^2F_{5/2} \rightarrow 4f\ ^2F_{7/2}$	12500000	17.8540	-1.0507	16.8033	1.8516	0.0001	1.8517

TABLE IV. Calculated lifetimes using the relativistic coupled-cluster (RCC) theory of some low-lying states in 10^{-9} sec along with their comparisons with the other theoretical (Others) and experimental (Exp) results.

State	RCC	RMBPT[c]	Others	Exp
$5p\ ^2P_{1/2}$	1.78	1.84	1.26[a]	1.45 ± 0.10[b], 1.72 ± 0.07[d]
$5p\ ^2P_{3/2}$	1.42	1.45		1.50 ± 0.15[d]
$6s\ ^2S_{1/2}$	0.65			
$5d\ ^2D_{3/2}$	0.53	0.67	0.56[a]	0.75 ± 0.06[d]
$5d\ ^2D_{5/2}$	0.58	0.61		0.98 ± 0.10[b], 0.58 ± 0.05[d]
$6p\ ^2P_{1/2}$	4.40			
$6p\ ^2P_{3/2}$	4.54			
$4f\ ^2F_{5/2}$	1.70	1.82		1.70 ± 0.07[d]
$4f\ ^2F_{7/2}$	1.72	1.74		1.72 ± 0.07[d]
$7s\ ^2S_{1/2}$	1.03			
$5g\ ^2G_{7/2}$	2.65			
$5g\ ^2G_{9/2}$	2.66	2.71		2.84 ± 0.30[d]

$a \rightarrow$ Relativistic Hartree Fock (RHF): [32];
$b \rightarrow$ Beam Foil: [29];
$c \rightarrow$ RMBPT: [30];
$d \rightarrow$ Beam Foil: [46];

TABLE V. Calculated hyperfine A constants along with the different correlation contributing terms in MHz.

State	d	$\overline{d}$	$\overline{d}S_1$	$\overline{d}S_2$	$S_1\overline{d}S_1$	$S_1\overline{d}S_2$	$S_2\overline{d}S_2$	Norm.	RCC
$5s\ ^2S_{1/2}$	17672.45	17635.18	2392.83	1382.51	81.21	72.73	345.29	-395.71	21358.30
$5p\ ^2P_{1/2}$	3317.77	3315.07	576.20	218.52	25.13	17.50	48.24	-66.76	4107.07
$5p\ ^2P_{3/2}$	514.01	518.29	89.92	68.51	3.92	5.10	22.45	-10.91	693.70
$6s\ ^2S_{1/2}$	4792.83	4779.14	318.36	340.26	5.32	2.40	106.62	-47.66	5467.19
$5d\ ^2D_{3/2}$	97.59	100.98	19.73	22.30	0.99	1.40	5.26	-1.16	149.53
$5d\ ^2D_{5/2}$	41.01	42.38	8.24	11.11	0.41	0.66	0.33	-0.49	62.63
$6p\ ^2P_{1/2}$	1090.79	1089.88	97.20	76.63	2.22	2.27	12.99	-11.97	1262.70
$6p\ ^2P_{3/2}$	173.61	174.80	16.01	23.18	0.38	0.53	11.54	-2.11	223.49
$4f\ ^2F_{5/2}$	2.60	2.65	0.48	-2.52	0.03	-0.24	1.73	-0.01	2.14
$4f\ ^2F_{7/2}$	1.45	1.49	0.27	-3.32	0.02	-0.41	0.03	0.01	-1.91
$7s\ ^2S_{1/2}$	2234.71	2227.97	-0.49	153.23	0.01	-4.34	53.48	-16.63	2396.80

TABLE VI. Calculated hyperfine B constants along with the different correlation contributing terms in MHz.

State	d	$\overline{d}$	$\overline{d}S_1$	$\overline{d}S_2$	$S_1\overline{d}S_1$	$S_1\overline{d}S_2$	$S_2\overline{d}S_2$	Norm.	RCC
$5p\ ^2P_{3/2}$	648.57	651.06	113.13	138.88	4.94	6.17	10.05	-14.25	905.47
$5d\ ^2D_{3/2}$	41.02	42.56	8.32	45.33	0.42	1.76	-0.06	-0.76	97.57
$5d\ ^2D_{5/2}$	55.79	57.76	11.22	63.38	0.56	2.43	-0.30	-1.04	134.00
$6p\ ^2P_{3/2}$	219.07	219.75	20.19	41.75	0.47	0.37	3.51	-2.66	282.32
$4f\ ^2F_{5/2}$	1.76	1.86	0.34	28.28	0.03	1.30	-0.30	-0.15	31.36
$4f\ ^2F_{7/2}$	2.06	2.17	0.40	33.15	0.03	1.53	-0.31	-0.18	36.79
$5g\ ^2G_{7/2}$	0.31	0.31	0.00	7.08	0.00	0.04	-0.05	0.00	7.39
$5g\ ^2G_{9/2}$	0.33	0.33	0.00	7.73	0.00	0.05	-0.05	0.00	8.06

TABLE VII. Hyperfine splitting (Spl) of the ground and few low lying excited states in MHz. The percentage contribution from the B constant (B-Cont) to these splitting are presented at the last column.

State	$F_1 \leftrightarrow F_2$	Spl	B-Cont
$5s\ ^2S_{1/2}$	$5 \leftrightarrow 4$	106791.51	0
$5p\ ^2P_{1/2}$	$5 \leftrightarrow 4$	20535.37	0
$5p\ ^2P_{3/2}$	$6 \leftrightarrow 5$	4765.84	12.67
	$5 \leftrightarrow 4$	3279.86	-5.75
$6s\ ^2S_{1/2}$	$5 \leftrightarrow 4$	27335.95	0
$5d\ ^2D_{3/2}$	$6 \leftrightarrow 5$	962.22	6.76
	$5 \leftrightarrow 4$	727.31	-2.79
$5d\ ^2D_{5/2}$	$7 \leftrightarrow 6$	500.92	12.48
	$6 \leftrightarrow 5$	385.81	2.61
$6p\ ^2P_{1/2}$	$5 \leftrightarrow 4$	6313.48	0
$6p\ ^2P_{3/2}$	$6 \leftrightarrow 5$	1529.17	12.31
	$5 \leftrightarrow 4$	1058.64	-5.56
$7s\ ^2S_{1/2}$	$5 \leftrightarrow 4$	11984.02	0

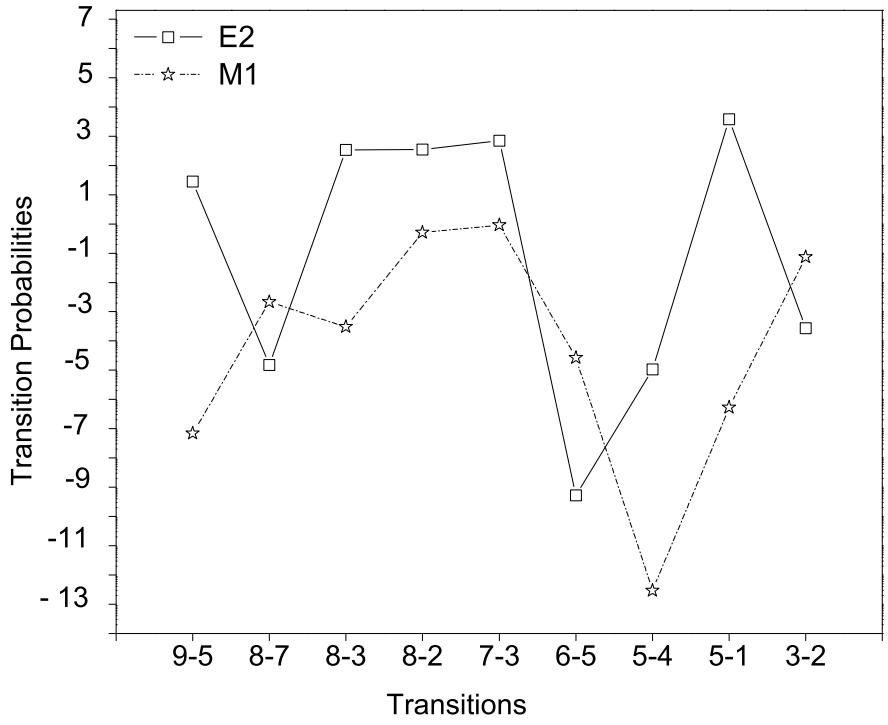

FIG. 1. Comparison between E2 and M1 transition probabilities (sec^{-1}) in the log_{10} scale.
The transitions between levels are presented along x- axis and the transition probabilities are presented along y-axis, the levels are identified as 1: $5s\ ^2S_{1/2}$, 2: $5p\ ^2P_{1/2}$, 3: $5p\ ^2P_{3/2}$, 4: $6s\ ^2S_{1/2}$, 5: $5d\ ^2D_{3/2}$, 6: $5d\ ^2D_{5/2}$, 7: $6p\ ^2P_{1/2}$, 8: $6p\ ^2P_{3/2}$, 9: $7s\ ^2S_{1/2}$

TABLE VIII. Hyperfine anomaly of In III.

State	A (113)	A (115)	A (117)	$^{113}\Delta^{115}(\%)$	$^{115}\Delta^{117}(\%)$
$5s^2S_{\frac{1}{2}}$	21313.0636	21358.3017	21271.3821	0.007491126	0.009042670
$6s^2S_{\frac{1}{2}}$	5455.6089	5467.1903	5444.9430	0.007461625	0.009008028
$7s^2S_{\frac{1}{2}}$	2391.7256	2396.8034	2387.0509	0.007438228	0.008981253
$5p^2P_{\frac{1}{2}}$	4098.0919	4107.0750	4090.7031	0.000558990	0.000676622
$5p^2P_{\frac{3}{2}}$	692.1824	693.6997	690.9345	0.000553917	0.000670590
$6p^2P_{\frac{1}{2}}$	1259.9349	1262.6970	1257.6639	0.000534891	0.000641958
$6p^2P_{\frac{3}{2}}$	223.0038	223.4925	222.6013	0.000642552	0.000779395

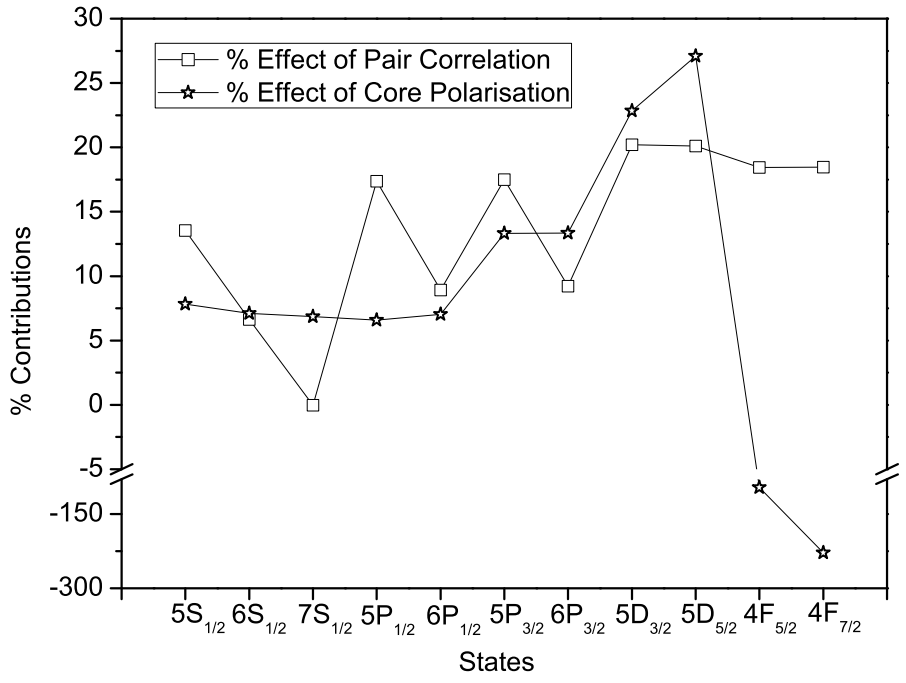

FIG. 2. Percentage contributions of the core polarization and pair correlation to the A constants.

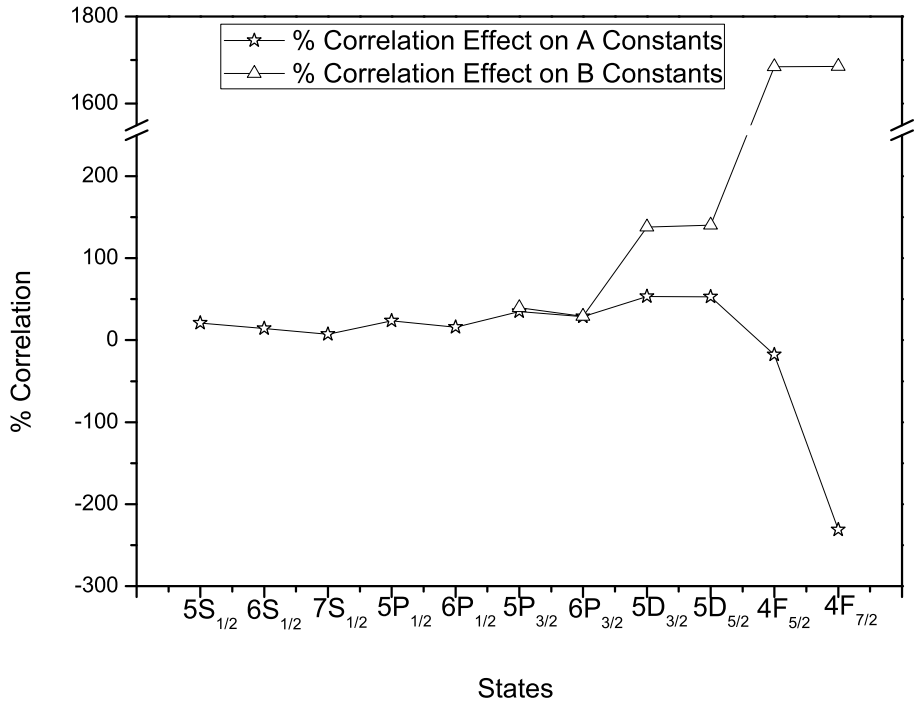

FIG. 3. Percentage values of correlation to the hyperfine A and B constants.

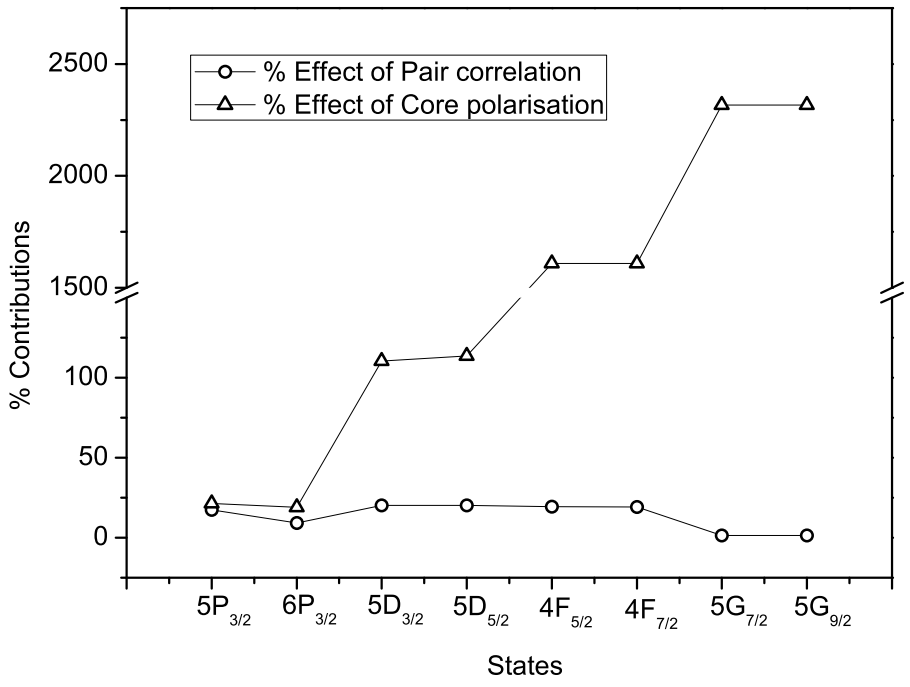

FIG. 4. Percentage contributions of the core polarization and pair correlation to the B constants.

[1] M. M. Schauer, J. R. Danielson, D. Feldbaum, M. S. Rahaman, L. B. Wang, J. Zhang, X. Zhao, and J. R. Torgerson, Phys. Rev. A **82**, 062518 (2010).

[2] B. M. Jelenkovic, S. Chang, J. D. Prestage, and L. Maleki, Phys. Rev. A **74**, 022505 (2006).

[3] G. Dixit, H. S. Nataraj, B. K. Sahoo, R. K. Chaudhuri, and S. Majumder, Phys. Rev. A **77**, 012718 (2008).

[4] M. Gunawardena, H. Cao, P. W. Hess, and P. K. Majumder, Phys Rev. A **80**, 032519 (2009).

[5] T G Eck, A Lurio, P Kusch, Phys. Rev, **106** 954 (1957).

[6] A. K. Mann And P. Kusch, phys. rev, **71**, 4 (1950).

[7] M. Das, R. K. Chaudhuri, S. Chattopadhyay and U. S. Mahapatra,J. Phys. B: At. Mol. Opt. Phys. **44**,065003 (2011).

[8] U. I. Safronova, M. S. Safronova, M. G. Kozlov, Phys Rev. A **76**, 022501 (2007).

[9] P. Raghavan, At. Data. Nucl. Data Tables **42**, 189 (1989).

[10] E. N. Fortson, Y. Pang and L. Wilets, Physical rev. Letter **65**, 23 (1990).

[11] A. Marie, M. Pendrill, Hyperne Interactions **127** 41 (2000).

[12] J R C Lopez-Urrutia,P. Beiersdorfer, K. Widmann, B. B. Birkett, A.-M. Martensson-Pendrill and M. G. H. Gustavsson, Phys. Rev. A, **57**, 879 (1998).

[13] S H Devare, H. G. Devare, F Pleiter, F C Magendans and L Niesen, Hyperfine Interactions, **15/16**, 31 (1983).

[14] J R Persson, Atomic Data and Nuclear Data tables, **99**, 62 (2013).

[15] O. Lutz, A. Nolle, and A. Uhl, Z. Physik 248, 159 (1971).

[16] A. Bohr, V.F. Weisskopf, Phys. Rev. **77**, 94 (1950).

[17] S. Buettgenbach, Hyperfine Int, **20**, 1 (1984).

[18] H.H. Stroke, H.T. Duong and J. Pinard, Hyperfine Int., **129**, 319 (2000)

[19] S. Djenie, A. Srekovi, S. Bukvi, Spectrochimica Acta Part B, **61**, 588 (2006).

[20] Z. Simic, M. S. Dimitrijevic, A. Kovacevic and S. Sahal-Brechot, Baltic Astronomy, **20**, 613 (2011).

[21] Cowley C R, Hartoog M R and Cowley A P, Astrophys. J. **194**, 343 (1974).

[22] N. Vitas, I. Vince, M. Lugaro, O. Andriyenko, M. Gosic and R. J. Rutten, Mon. Not. R. Astron. Soc. **384**, 370 (2008).

[23] M. Skocic, M. Burger, S. Bukvic and S. Djenize, J. Phys. B: At. Mol. Opt. Phys. **45**, 225701 (2012).

[24] Djenize S, Sreckovic A and Bukvic S, Spectrochim. Acta B **61**, 588 (2006).

[25] Dimitrijevic M, Kovacevic A, Simic Z and Sahal-Brechot S Balt. Astron. **20** 495 (2011).

[26] M. A. Ali, and Yong-Ki Kim, Phys. Rev. A **38**, 3992 (1988).

[27] Nodwell R A, PhD Thesis University of British Columbia, Vancouver (1956).

[28] K S Bhatia, J. Phys. B: Atom. Molec. Phys., **11**, 14 (1978).

[29] T. Andersen, A. Kirkegard Nielsen and G. Sorensen, Physica Scripta. **6**, 122 (1972).

[30] U. I. Safronova, I. M. Savukov, M. S. Safronova, W. R. Johnson, Physical Review A **68**, 062505 (2003).

[31] L. Gowacki and J. Migdaek, Phys. Rev. A **80**, 042505 (2009).

[32] Kwok-tsang Cheng and Yong-Ki Kim,J. Opt. Soc. Am., **69**, 1 (1979).

[33] I. Martin, M. A. Almaraz, C. Lavin,Z. Phys. D **35**, 239 (1995).

[34] Xiao-Bin Ding, F. Koike, I. Murakami, D. Kato,H. A Sakaue, Chen-Zhong Dong and N. Nakamura J. Phys. B: At. Mol. Opt. Phys. **45**, 035003 (2012).

[35] N. N. Dutta, and S. Majumder, Phys. Rev. A **85**, 032512 (2012).

[36] N. N. Dutta, and S. Majumder, Astrophys. J. **737**, 25 (2011).

[37] R. F. Bishop, and H. G. Kummel, Phys. Today, March **40**, 52 (1987).

[38] I. Lindgren, and D. Mukherjee, Phys. Rep 151, 93 (1987).

[39] R. K. Chaudhuri, B. K. Sahoo, B. P. Das, H. Merlitz, U. S. Mahapatra, and D. Mukherjee, J. Chem. Phys. 119, 10633 (2003).

[40] A. Szabo and N. S. Ostlund, *Modern Quantum Chemistry: Introduction to Advanced Electronic Structure Theory* (Dover Publications, Mineola, 1996).

[41] N. N. Dutta,S. Roy, G. Dixit, S. Majumder, Phys Rev. A **87**, 012501 (2013).

[42] O. Lutz, A. Nolle, and A. Uhl, Z. Physik **248**, 159 (1971).

[43] N. N. Dutta, and S. Majumder, Phys. Rev. A **88**, 062507 (2013)

[44] NIST Atomic Spectra Database (ver.5.0), [Online]. Available: http://physics.nist.gov/asd [2012, August 1]. National Institute of Standards and Technology, Gaithersburg, MD.

[45] J Migdalek and M Garmulewicz,J. Phys. B: At. Mol. Opt. Phys. **33**, 1735 (2000).

[46] W. Ansbacher, E.H.Pinnington, J. A. Kernahan, R. N. Gosselin, Can. J. Phys. **64**, 1365 (1986).

[47] G Dixit, B. K. Sahoo, R. K. Chaudhuri and S. Majumder, Phys. Rev. A **76**, 042505 (2007).

[48] P. Sancho, Arxiv:1311.0998 (2013).

[49] S. Bttgenbach, Hyperfine Int. **20** 1 (1984).

[50] A. Owusu, X. Yuan, S. N. Panigrahy, R. W. Dougherty, and T. P. Das, Phys. Rev. A **55**, 4 (1997).

[51] H.S. Chou and W.R. Johnson, Phys. Rev. A **56**, 2424 (1997).